2017.6.5 - 6.8
7th APTWG International Conference
Nagoya University, Nagoya, Japan
D-O1

ITB formation by toroidal momentum injection in flux-driven gyrokinetic turbulence

Contents

Kenji Imadera[1), Jiquan Li[2) and Yasuaki Kishimoto[1)

1) Graduate School of Energy Science, Kyoto University, Japan
2) Southwestern Institute of Physics, China

Background: ITB Formation in Weak/Revered Magnetic Shear Plasma

- ✓ ITB is formed in the recent HL-2A weak magnetic shear discharges. They found that mean flow triggered by toroidal rotation plays a dominant role in sustaining ITB.
- ✓ Clear box-type ITB is formed in the JT-60U reversed shear discharges, in which co-input is more beneficial for ITB formation than counter-input.

HL-2A (weak shear, Co)

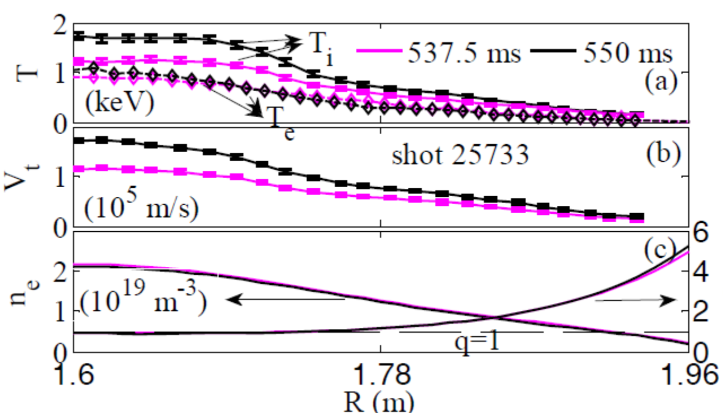

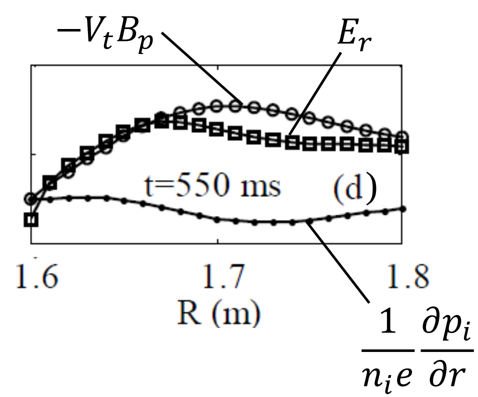

$$E_r = -V_t B_p + V_p B_t + \frac{1}{n_i e}\frac{\partial p_i}{\partial r}$$

[D. L. Yu, *et al.*, EX/8-2, 26th IAEA-FEC (2016).]

JT-60U (reversed shear, Co)

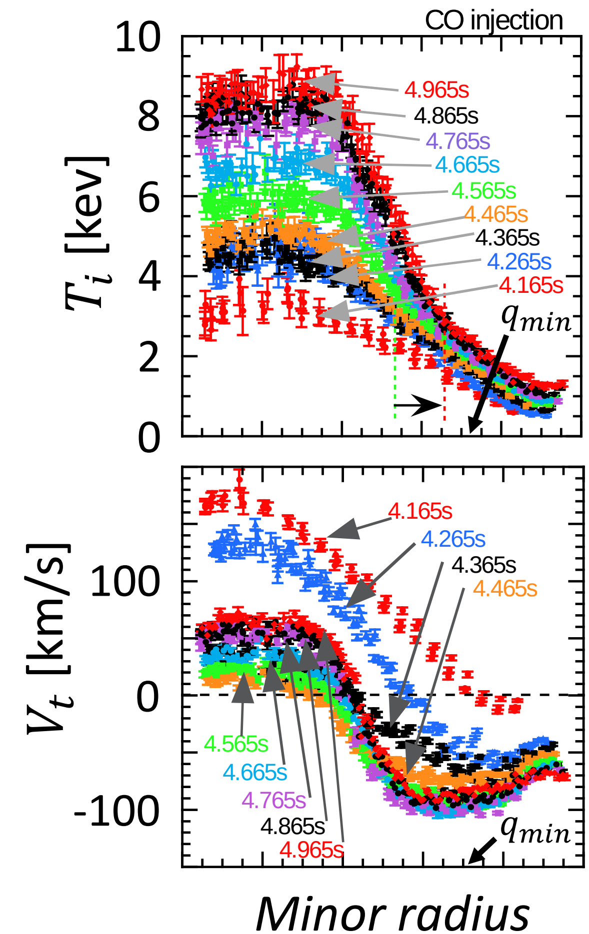

[Courtesy of Y. Sakamoto, QST]

Purpose of This Work

Purpose of this work

✓ Understanding the underlying mechanism of ITB formation in global gyrokinetic ITG turbulence

Radial force balance

$$E_r = -\frac{T_i}{e}\left(\frac{1}{L_{n_i}} + \frac{1-k}{L_{T_i}}\right) + \frac{rB}{qR}U_{\parallel}$$

Approaches

1. Non-local first-order ballooning theory
   - ✓ Notation of θ_b, Δr and γ
   - ✓ Impact of mean flow

2. Linear/Nonlinear global GK ITG simulation
   - ✓ Impact of mean flow

3. Toroidal momentum injection
   - ✓ Impact of toroidal momentum injection
   - ✓ Hysteresis nature in the modulation test

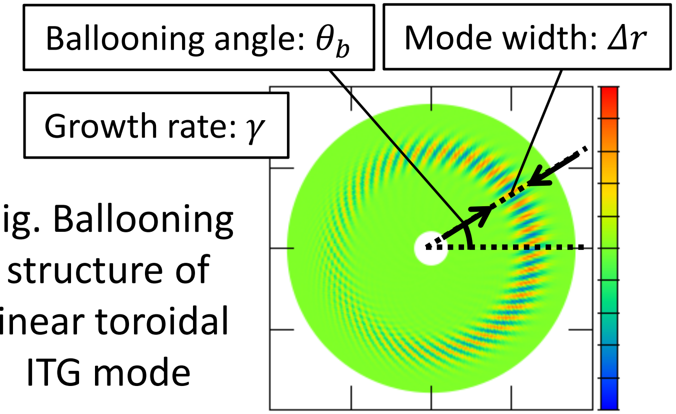

Fig. Ballooning structure of linear toroidal ITG mode

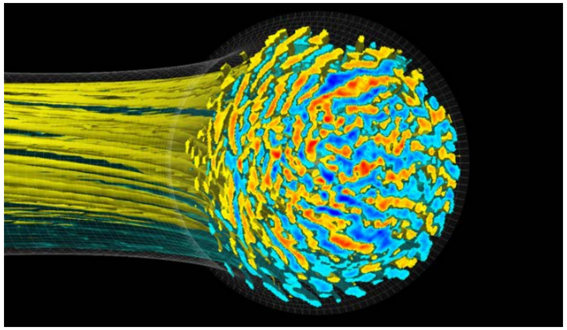

Fig. Typical structure of flux-driven toroidal ITG turbulence calculated by *GKNET*

Non-Local Ballooning Theory

[Y. Kishimoto, *et.al.*, Plasmas Phys. Controlled Fusion **40**, A663 (1998).]

$$\theta_b = \mp \left| \frac{\partial_r(\omega_r + \omega_f)}{2k_\theta \gamma_0 \hat{s}} \right|^{1/3}$$

$$\Delta r = \left| \frac{\sin\theta_b}{k_\theta^2 \hat{s}^2 \theta_b^3} \right|^{1/2}$$

$$\gamma = \gamma_0 \cos\theta_b$$

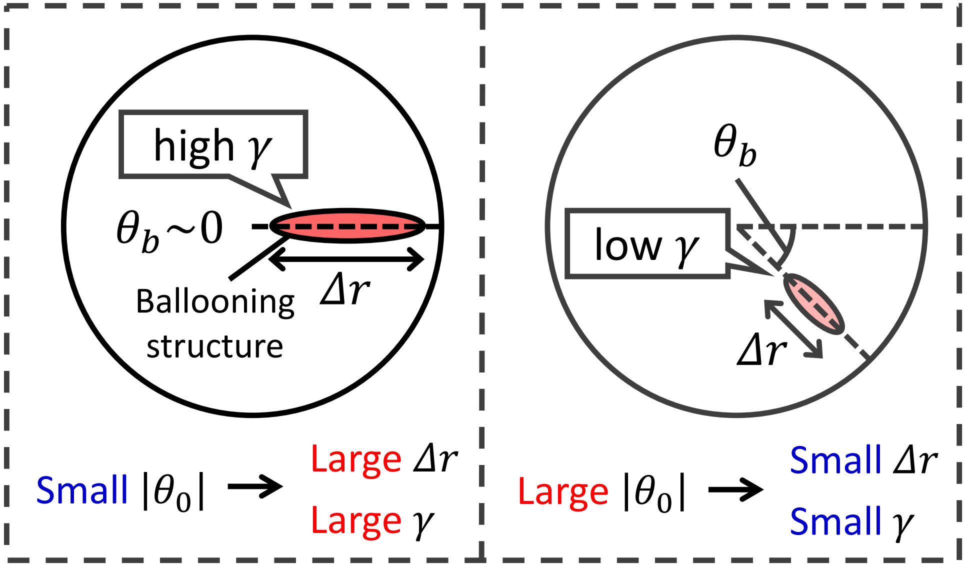

Radial force balance

$$E_r = \frac{rB}{qR} U_\parallel - \frac{T_i}{e}\left(\frac{1}{L_{n_i}} + \frac{1-k}{L_{T_i}}\right) \qquad \left(\begin{array}{l} n_i = n_{i0}\exp(-r/L_{n_i}) \\ T_i = T_{i0}\exp(-r/L_{T_i}) \end{array}\right)$$

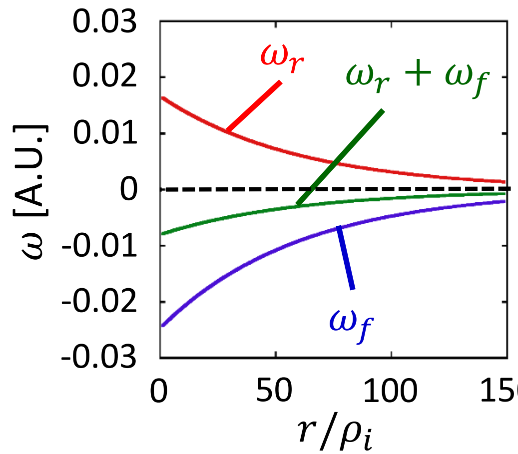

Eigenfrequency + Doppler shift frequency

$$\omega_r + \omega_f \sim \frac{k_\theta}{eB}\left[\left(\frac{2}{R_0} - \frac{1}{L_{n_i}} - \frac{1-k}{L_{T_i}}\right) T_i - \frac{erB}{qR} U_\parallel\right]$$

Diamagnetic drift *Mean flow* *Toroidal rotation*

✓ Cancellation by mean flow

✓ Impact of toroidal rotation

Nonlinear Flux-Driven GK ITG Simulation

Simulation condition

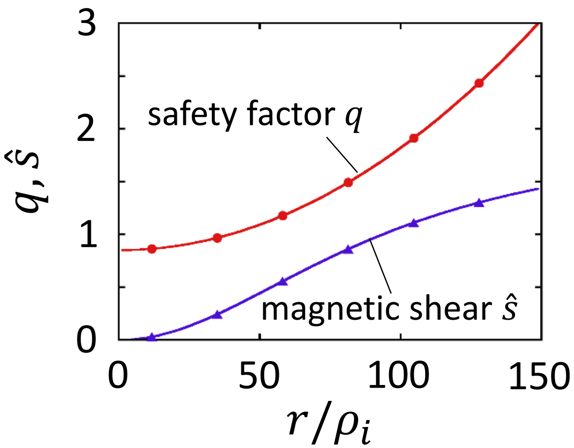

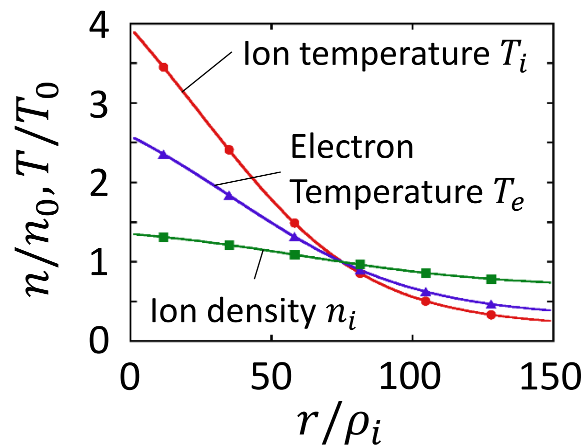

Parameter	Value
a_0/ρ_i	150
a_0/R_0	0.36
$(R_0/L_n)_{r=a_0/2}$	2.22
$(R_0/L_{T\,i})_{r=a_0/2}$	10.0
$(R_0/L_{T\,e})_{r=a_0/2}$	6.92
ν_*	0.28
P_{in}	4, 8, 16, 24 [MW]

Source operator

$$S_{src} = A_{src}(r)\tau_{src}^{-1}[f_M(2\bar{T}) - f_M(\bar{T})]$$

✓ Constant power input near magnetic axis

Sink operator

$$S_{snk} = A_{snk}(r)\tau_{snk}^{-1}[f(t) - f(t=0)]$$

✓ Krook-type operator to f in boundary region

[Y. Idomura, *et. al.*, Nucl. Fusion, **49**, 065029 (2009).]

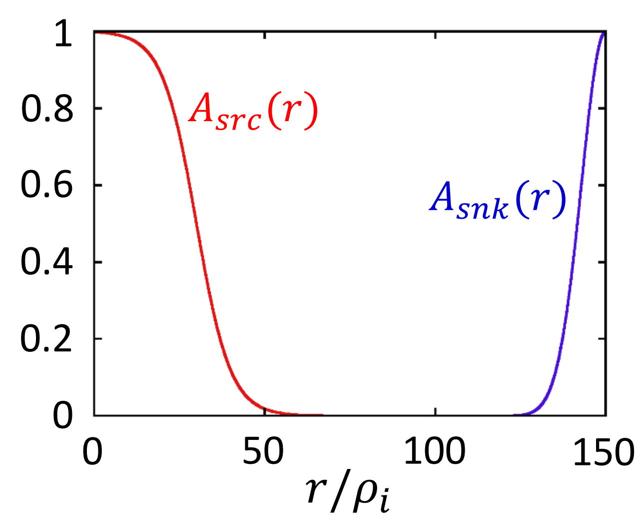

Poloidal Symmetry and Profile Stiffness

2D spatial correlation analysis for potential structure (16MW)

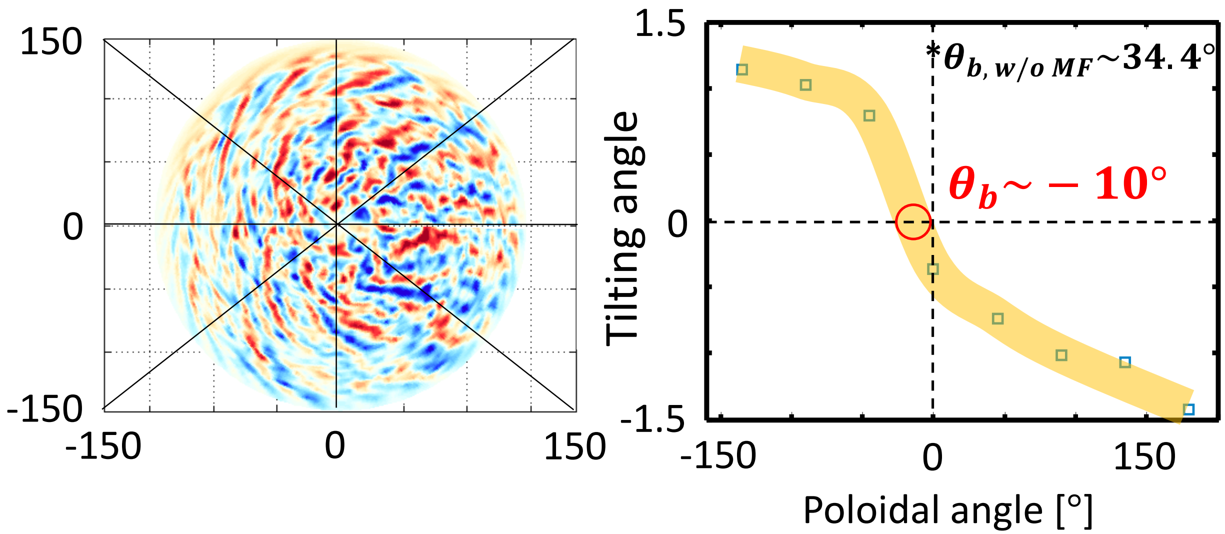

✓ Ballooning angle is smaller than that estimated from linear analysis without E_r.

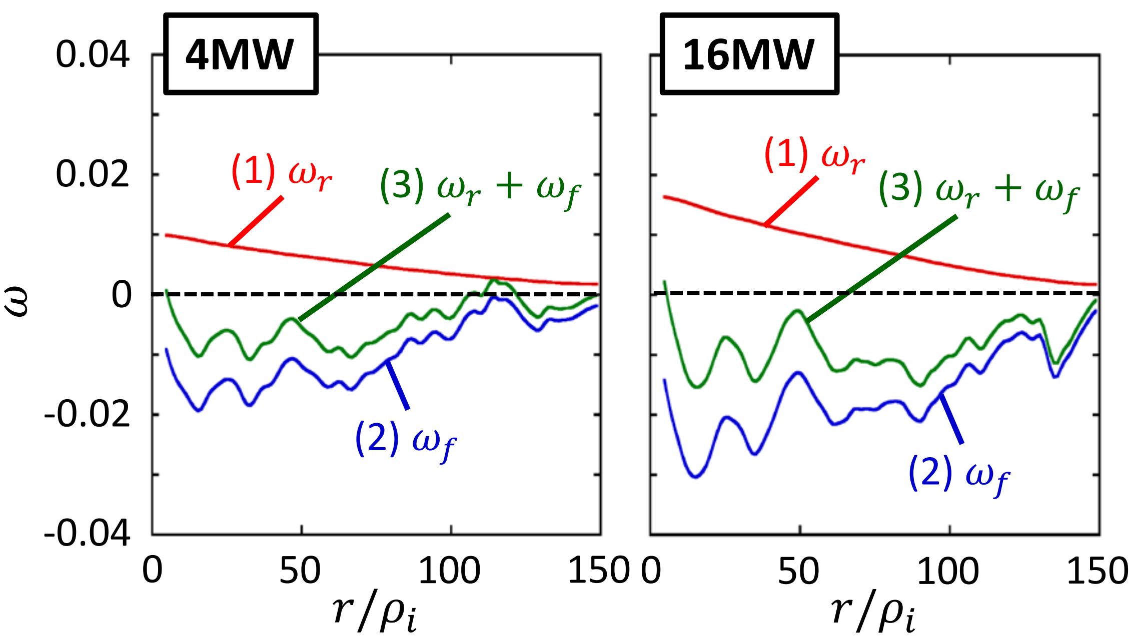

Gradient-Flux relation in power scan test

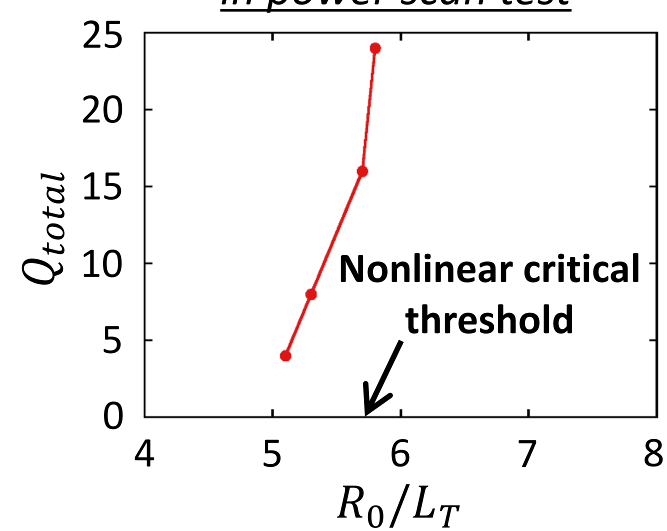

Flux-Driven ITG Simulation with Momentum Source by GKNET

Simulation condition

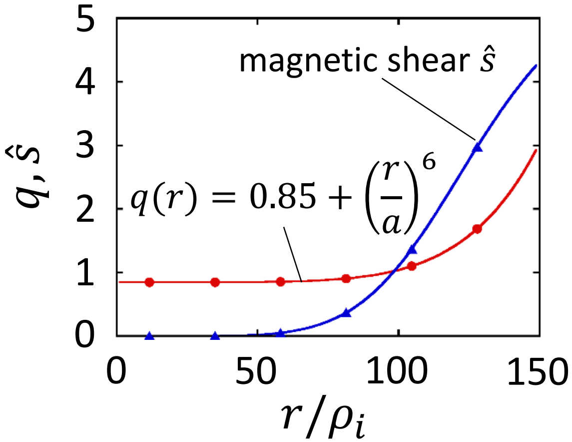

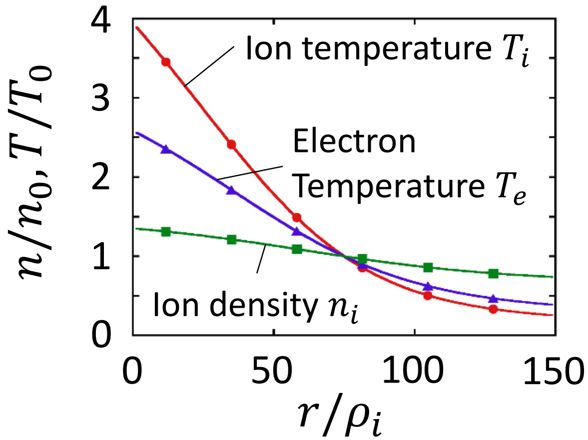

Parameter	Value
a_0/ρ_i	150
a_0/R_0	0.36
$(R_0/L_{n_i})_{r=a_0/2}$	2.22
$(R_0/L_{T_i})_{r=a_0/2}$	10.0
$(R_0/L_{T_e})_{r=a_0/2}$	6.92
ν_*	0.28
P_{in}	4 [MW]
T_{in}	11.2 [N・m]

Momentum source operator

$$S_M = \tau_M^{-1} A(r)[f_{LM}(n_0, 0.5v_{ti}, T_0) - f_{LM}(n_0, 0, T_0)]$$

$$f_{LM}(n, U_{||}, T) = \frac{n}{\sqrt{2\pi T^3/m_i^3}} exp\left[-\frac{0.5(v_\parallel - U_\parallel)^2 + \mu B}{T/m_i}\right]$$

✓ We compare three cases;

(A) without momentum source

(B) with co momentum source at $r = 0.6a$

(C) with counter momentum source at $r = 0.6a$

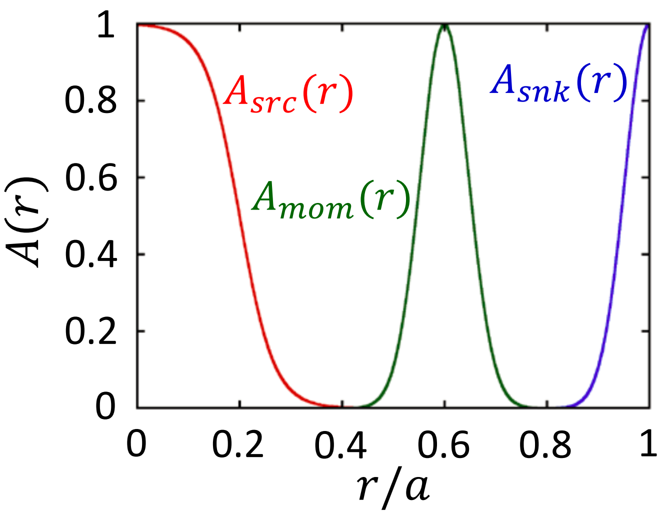

Effect of Rotation Direction

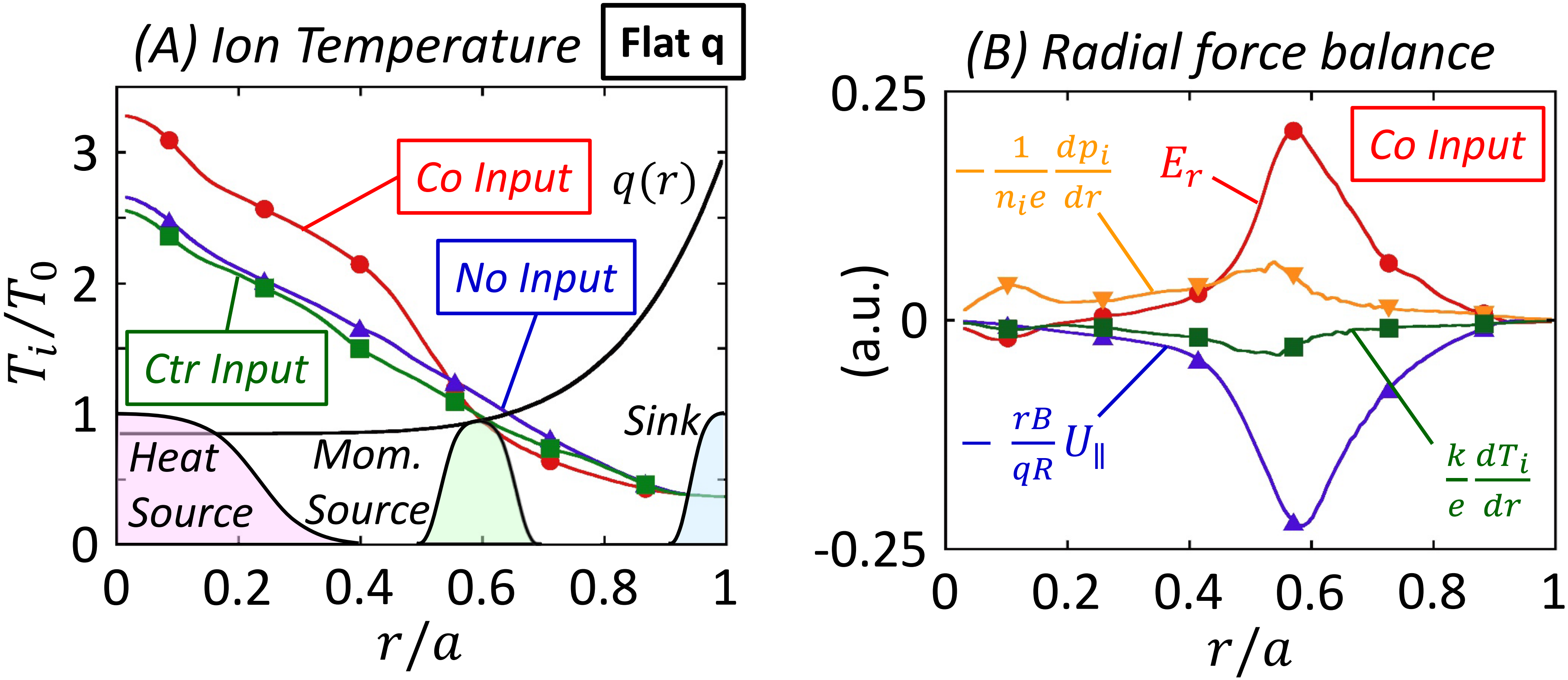

✓ Only co-current toroidal rotation can benefit the ITB formation in weak magnetic shear plasma.

→ qualitative agreement with the observations in the JET experiment

Feedback Loop between Mean E_r Shear and Momentum Pinch

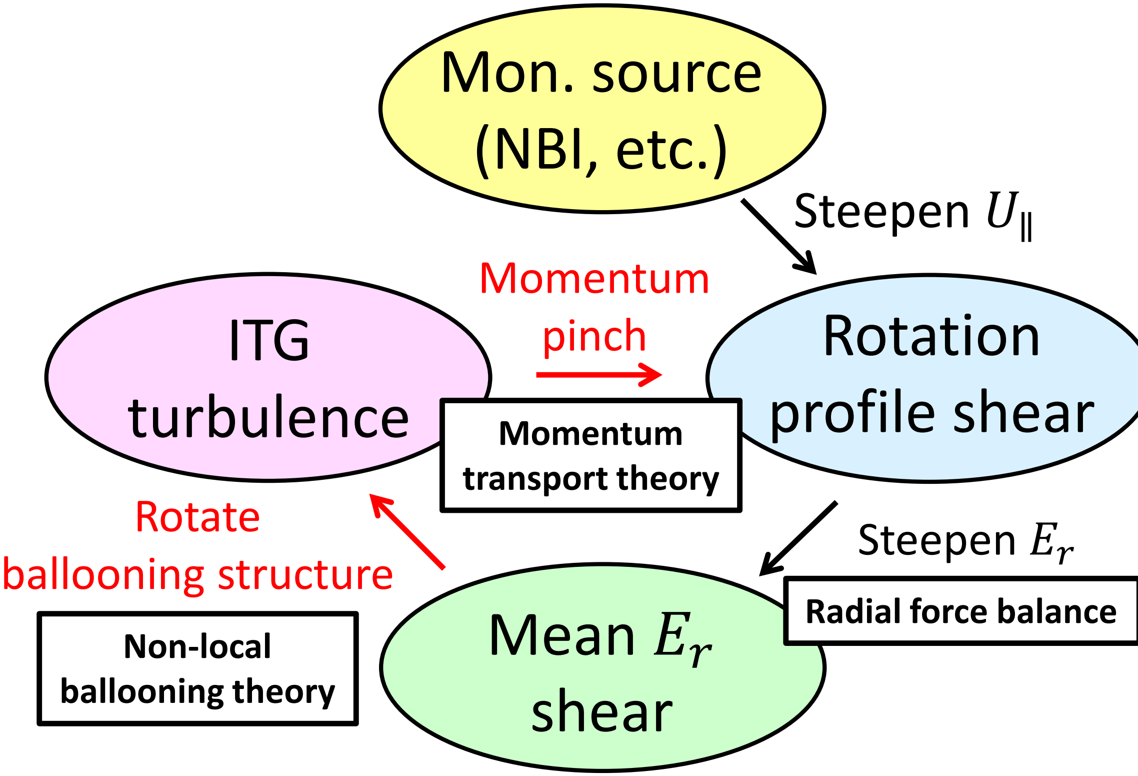

Momentum transport theory

$$R_\varphi \equiv \frac{\Gamma_\varphi^r}{Q_i^r}\frac{v_{ti}}{R_0} = \frac{2}{R/L_T}\frac{\chi_\varphi}{\chi_i}\left[u' + \frac{R_0 V_{co}}{\chi_\varphi}u + \frac{C^*}{\chi_\varphi}\right]$$

$$\frac{C^*}{\chi_\varphi} \sim -\frac{\hat{s}}{2qk_\theta\rho_{ti}}\left[\frac{R_0}{L_n} + 4\right]\theta_0$$

[Y. Camenen, *et al*. Nucl. Fusion **51**, 073039 (2011).]

Radial force balance

$$E_r + \frac{k}{e}\frac{\partial T_i}{\partial r} - \frac{rB}{qR}U_\parallel - \frac{1}{n_i e}\frac{\partial p_i}{\partial r} = 0$$

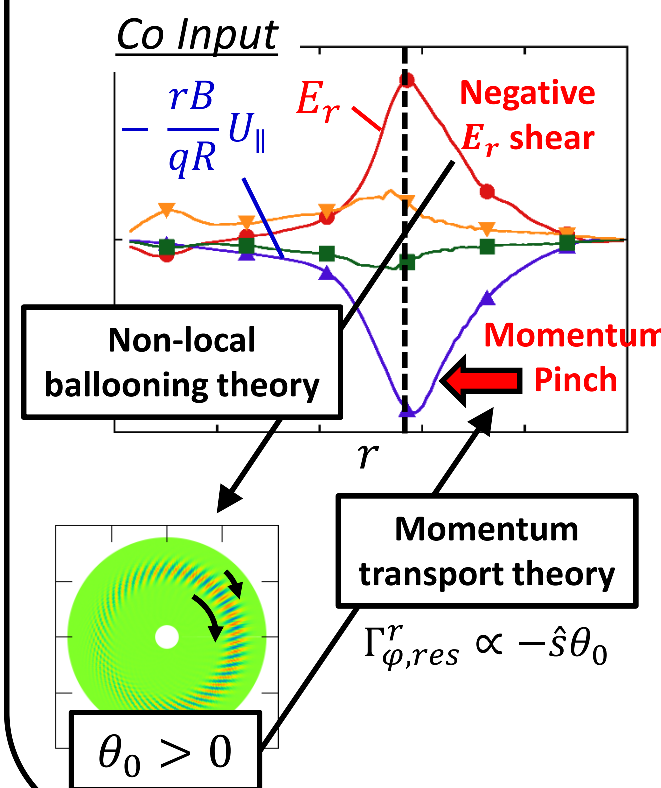

Summary & Future Plans - 1

Summary

- ✓ We found that a momentum source can change the mean E_r through the radial force balance, leading to ITB formation.
- ✓ The underlying mechanism is identified to originate from a positive feedback loop between the enhanced mean E_r shear and resultant momentum pinch, which can be observed only in co-input case.

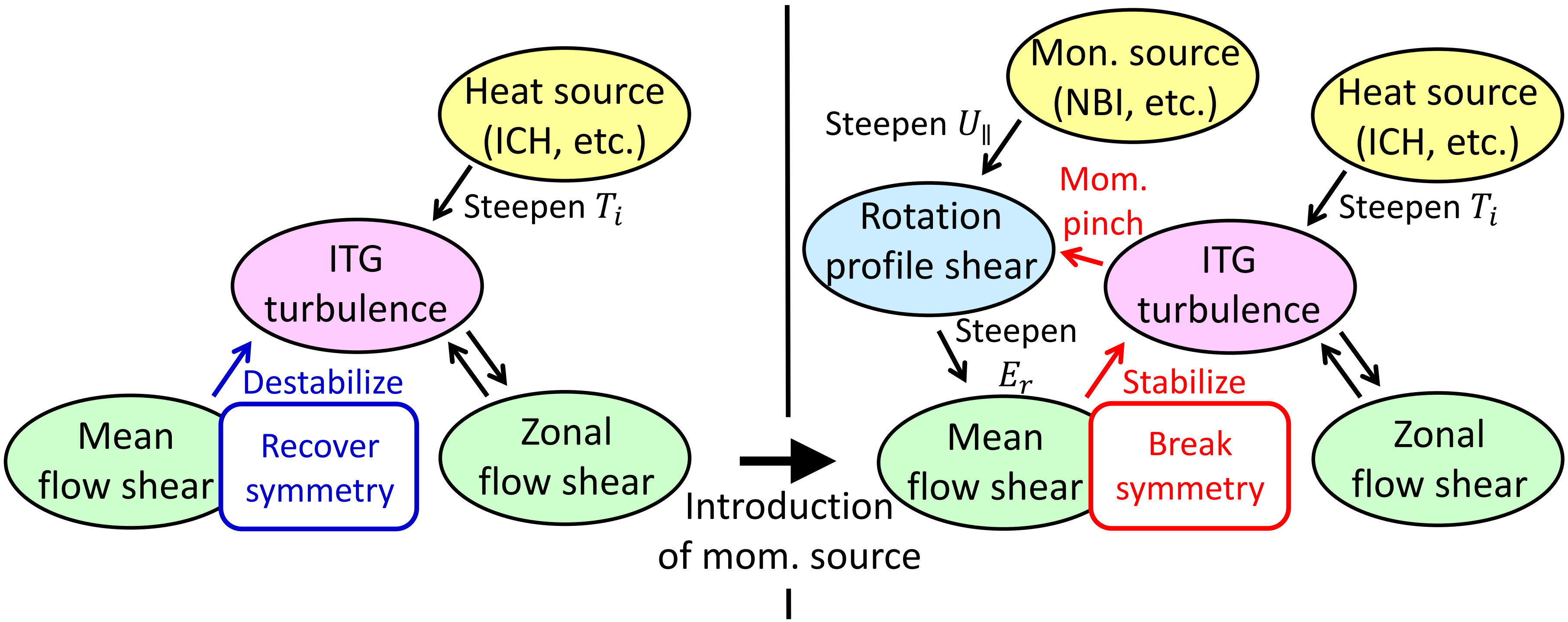

Summary & Future Plans - 2

Future plans

[K. Obrejan *et al*, Comput. Phys. Comm. **216**, 8 (2017).]

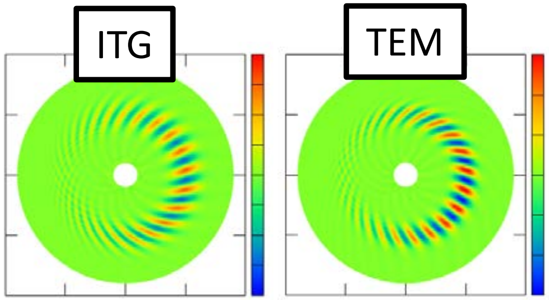

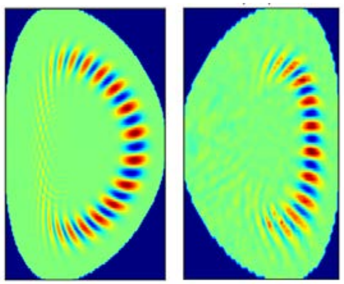

ITB formation in flux-driven ITG turbulence

Introduction of kinetic electron

Magnetic shaping effect on ZF/GAM dynamics

ITB formation in flux-driven ITG/TEM turbulence

- ✓ Opposite ballooning angle
- ✓ Density transport
- ✓ Momentum transport

Magnetic shaping effect on ITG/TEM instability

- ✓ Impact of elongation and triangularity on ITG/TEM turbulence

Control of barrier formation by multi-sources and magnetic shape